In the search for footprints of strangelets at the Himalaya Mountains

Rupamoy Bhattacharyya

Bose Institute, Calcutta, India

Outline of the talk

- Introduction
- Status of the search for strangelets
  - in the accelerator experiments
  - in the cosmic radiation
- The search at the Himalayan mountains
- Conclusions

Strangelets

Strange Quark Matter (SQM):

Hypothetical bound state of large ($10<A<10^{56}$) but roughly equal numbers of up, down and strange quarks conjectured as the true ground state of nuclear matter .

Classification of SQM: Strangelets (***A*<10^6^**)

Nuclearite (***A*>10^6^**)

Nucleus

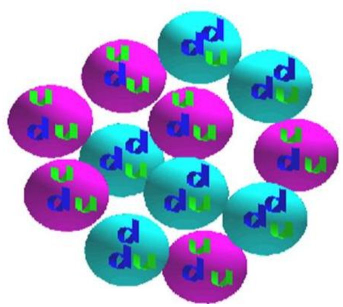

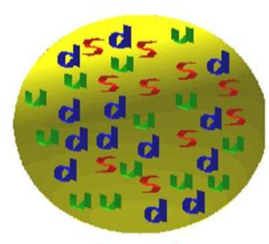

SQM

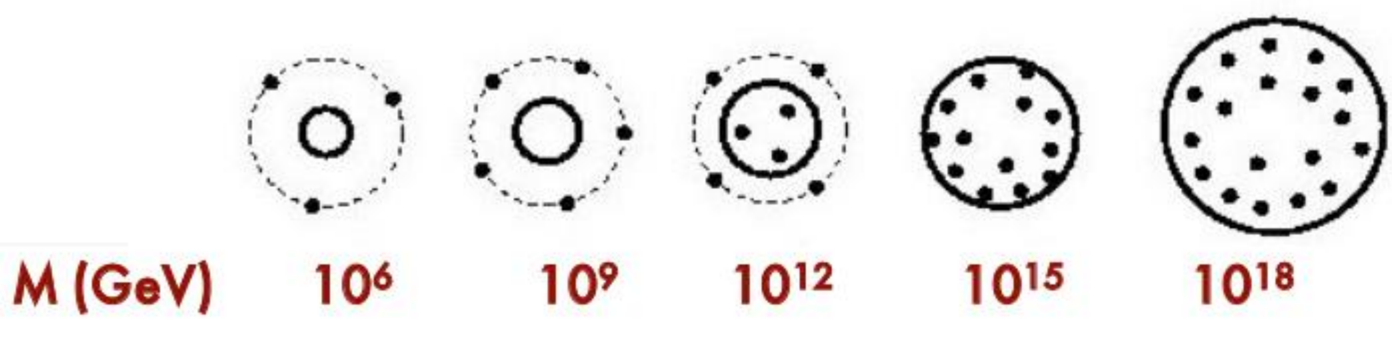

• electrons

Possible cosmological origin:

Strangelets may be produced at the early stage of the universe

Possible astrophysical origin:

collisions of two strange stars

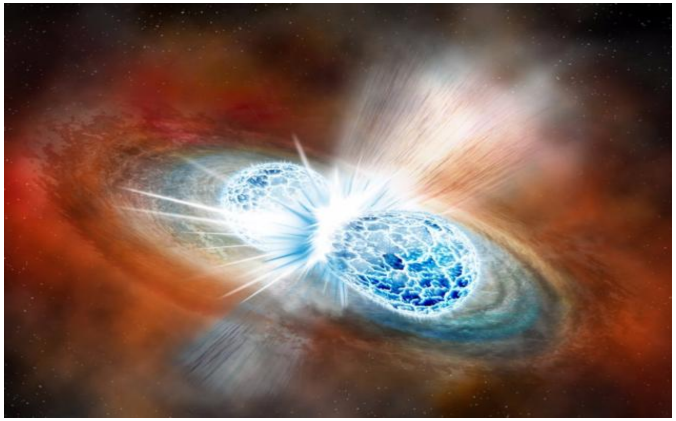

ejected in supernovae explosions

In man-made accelerators/ colliders:

- Relativistic Heavy Ion Collider (RHIC) at Brookhaven
- Large Hadron Collider (LHC) at CERN

Why strangelets may be more stable

A (The!) simple(est!!) calculation on "Strange matter Hypothesis"

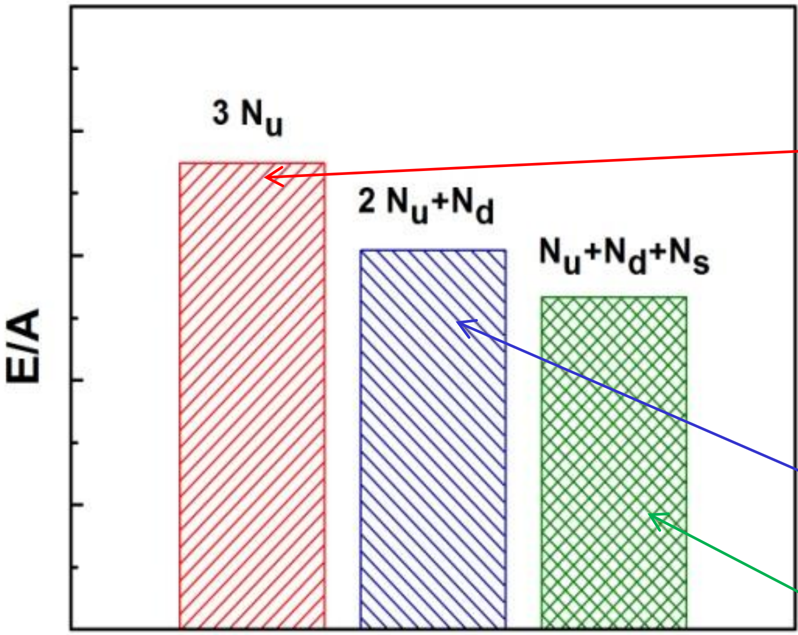

$$E_{N_u,N_d,N_s} < E_{2N_u,N_d} < E_{3N_u}$$

$$3N = 3N_u$$

$$E_{3N_u} = \frac{2\pi V c}{h^3}\left(\frac{N h^3}{8\pi V}\right)^{\frac{4}{3}} \times \left[9^{\frac{4}{3}}\right]$$

$$3N = 2N_u + N_d$$

$$E_{2N_u,N_d} = \frac{2\pi V c}{h^3}\left(\frac{N h^3}{8\pi V}\right)^{\frac{4}{3}} \times \left[6^{\frac{4}{3}} + 3^{\frac{4}{3}}\right]$$

$$3N = N_u + N_d + N_s$$

$$E_{N_u,N_d,N_s} = \frac{2\pi V c}{h^3}\left(\frac{N h^3}{8\pi V}\right)^{\frac{4}{3}} \times \left[3^{\frac{4}{3}} + 3^{\frac{4}{3}} + 3^{\frac{4}{3}}\right]$$

$m_u = m_d \approx 0$

$m_s \approx 95 \pm 5\,MeV/c^2$

+ other effects (surface tension, curveture...)

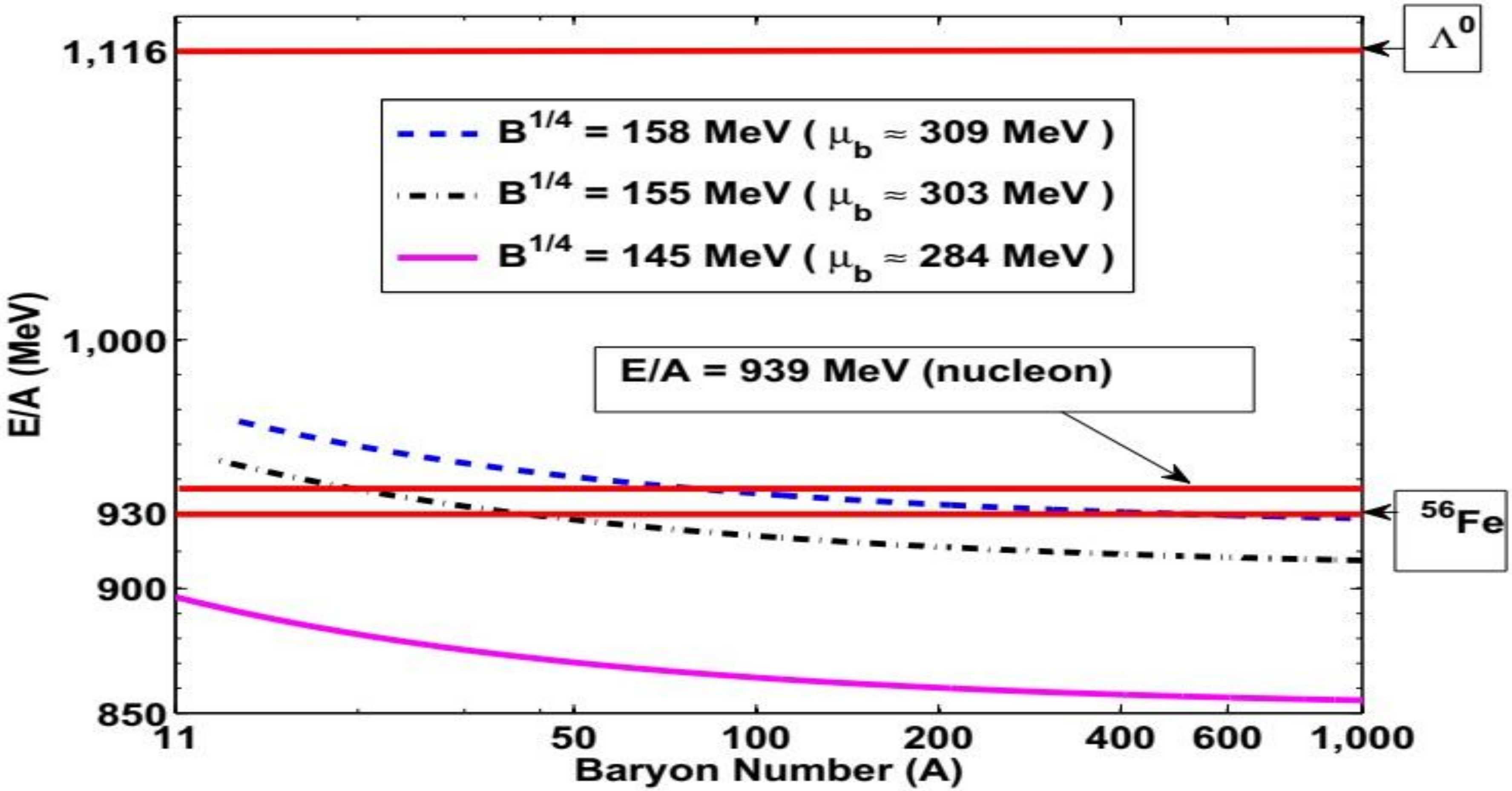

[Multifragmentation model for the production of astrophysical strangelets S Biswas, JN De, PS Joarder, S Raha, D Syam Physical Review C 95 (4), 045201]

Charge to mass ratio for strangelet

Ordinary strangelets

$$Z \approx 0.1\left(\frac{m_s}{150\,\mathrm{MeV}}\right)^2 A \qquad A<1000 \qquad (1)$$

$$Z \approx 8\left(\frac{m_s}{150\,\mathrm{MeV}}\right)^2 A^{\frac{1}{3}} \qquad A>1000 \qquad (2)$$

Color Flavor Locked strangelets

$$Z \approx 0.3\left(\frac{m_s}{150\,\mathrm{MeV}}\right) A^{\frac{2}{3}} \qquad (3)$$

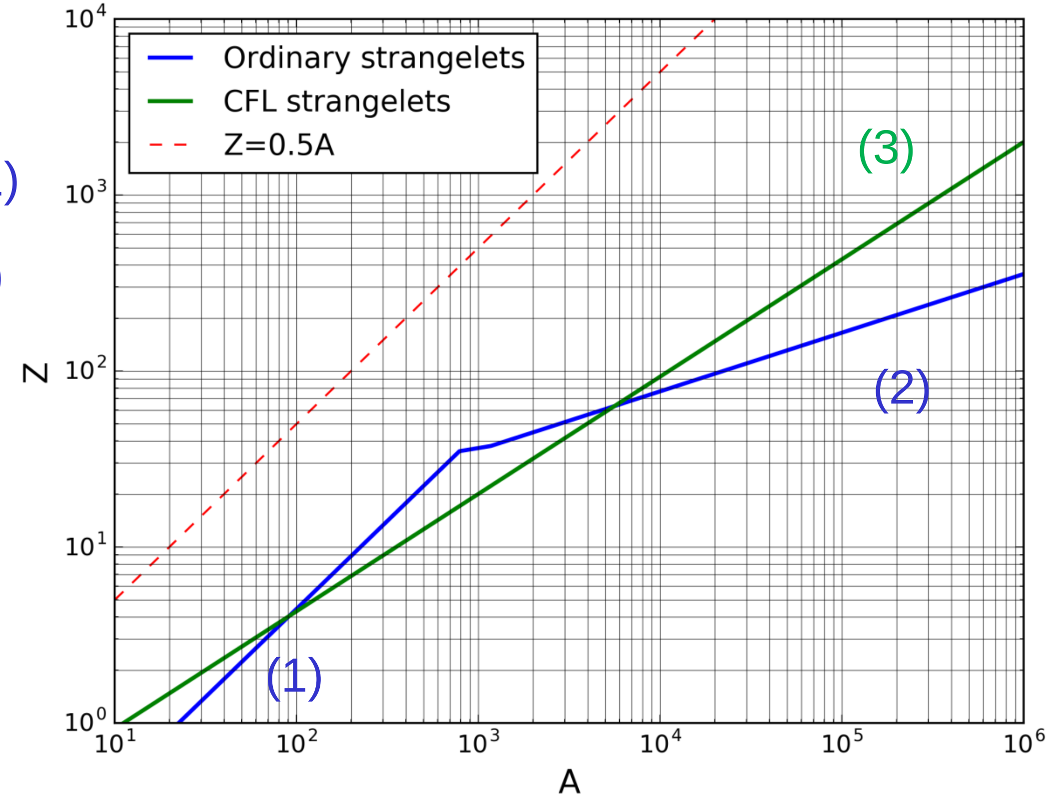

unique experimental signature of strangelets: unusually low charge to baryon number ratio (Z/A<<0.5) compared to ordinary nuclei.

Collider search for strangelet:
end of the Earth!!

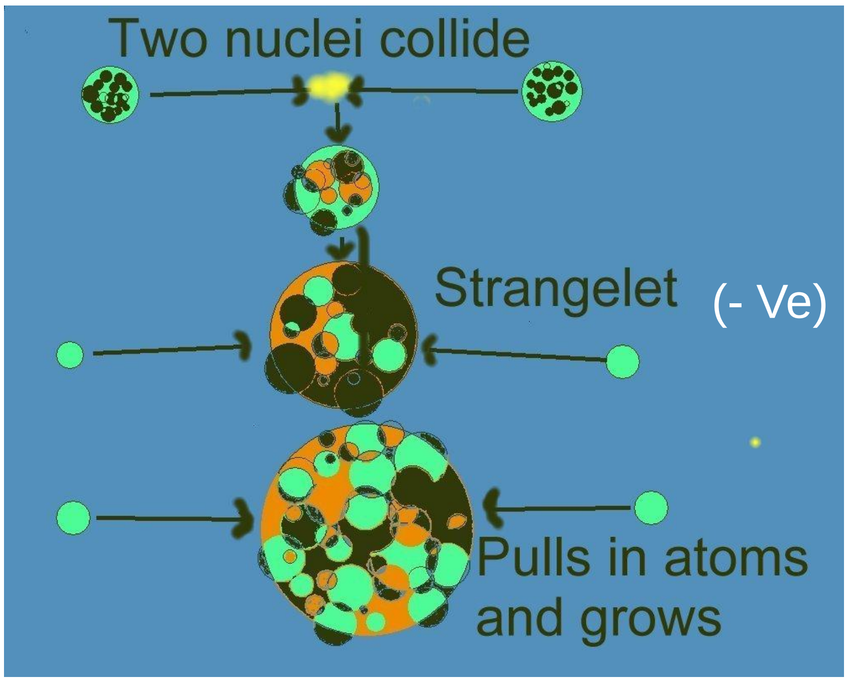

Newspaper report regarding the danger at LHC

https://www.nytimes.com/2008/03/29/science/29colli

The New York Times

SCIENCE

Asking a Judge to Save the World, and Maybe a Whole Lot More

By DENNIS OVERBYE MARCH 29, 2008

RELATED COVERAGE

TIMES TOPIC
CERN

Part of a detector to study results of proton collisions by a particle accelerator that a federal lawsuit filed in Hawaii seeks to stop. Valerio Mezzanotti for The New York Times

Scientific committee report

ELSEVIER

Physics Letters B

Volume 470, Issues 1–4, 16 December 1999, Pages 142-148

open access

Will relativistic heavy-ion colliders destroy our planet?

Arnon Dar ab, A. De Rújula a, Ulrich Heinz a

We conclude that, beyond reasonable doubt, heavy-ion experiments at RHIC will not endanger our planet.

(**Review of Speculative "Disaster Scenarios" at RHIC** W. Busza, R.L. Jaffe, J. Sandweiss and F. Wilczek ; Rev. Mod. Phys. 72, 1125 – Published 1 October 2000)

"There is no evidence whatsoever for stable strange matter anywhere in the Universe.

Strangelets small enough to be produced in heavy ion collisions are not expected to be stable enough to be dangerous

probability of producing a strangelet decreases very rapidly with the strangelet's atomic mass

It is overwhelmingly likely that the most stable configuration of strange matter has positive electric charge."

Strangelet search at accelerator

RHIC

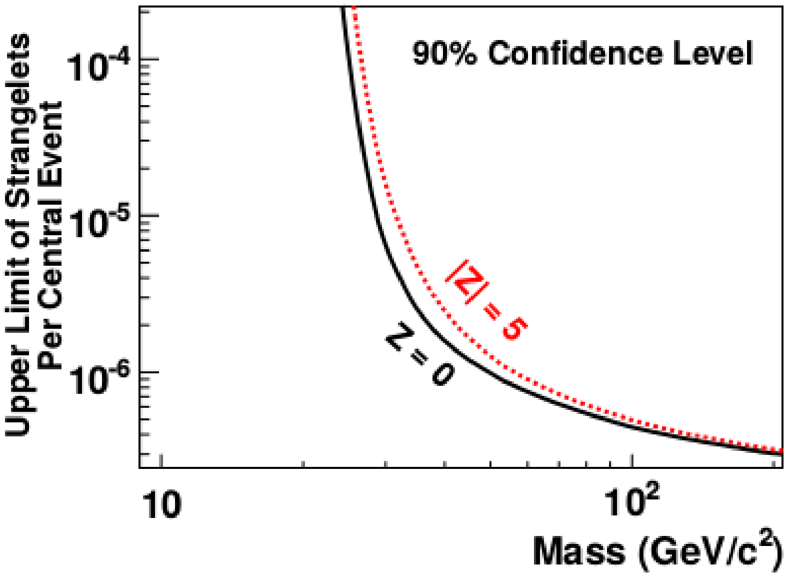

Strangelet search in Au+Au collisions at √sNN=200 GeV
B. I. Abelev et al. (STAR Collaboration) Phys. Rev. C 76, 011901(R) – Published 25 July 2007

LHC

An event with muonic bundles of high multiplicity observed by ALICE collaboration at **CERN** has been interpreted as probably due to disintegration of a strangelet

Muon bundles as a sign of strangelets from the universe
P. Kankiewicz, M. Rybczyński, Z. Włodarczyk and G. Wilk,, The Astrophysical Journal 839 (2017) 31

Reports of events with unusual Z/A ratio

There are several observations with unusual charge to mass ratio in different cosmic ray experiments.

- In 1990, Saito *et al.* analyzed the data of 1981 balloon borne experiment and claimed to have identified two events which were consistent with A ~ 370 and Z ~ 14 and was explained in the scheme of strange quark matter.
- In 1993 Ichimura *et al*. reported an event with unusually long m.f.p. called the 'exotic track' event with Z ~ 20 and A ~ 460. The report was based on an analysis of a 1989 balloon borne experiment using solid state nuclear track detector.
- In a paper in 2001 Fujii *et. al*. reported detection of a possible SQM candidate, an anomalous massive nuclei of charge Z~14 and M~370 amu in a hybdrid system combining active (Cherenkov and scintillation)and passive detectors (CR-39) in a 19 hr balloon flight.
- Analysis of data from AMS-01, has given hints of some interesting events, such as one with Z=2, A=8 [Aguilar *et.al*.(2002)]
- ultra-high-energy cosmic rays (UHECRs) detected through extensive air showers (EAS) might be associated with strangelets

Event	Charge	Baryon number	Atmospheric depth (g cm-2)
Counter experiment	14	370	13
Exotic track	20	460	200
Price's event	46	> 1000	3-5
AMS-01 event	8	54	0

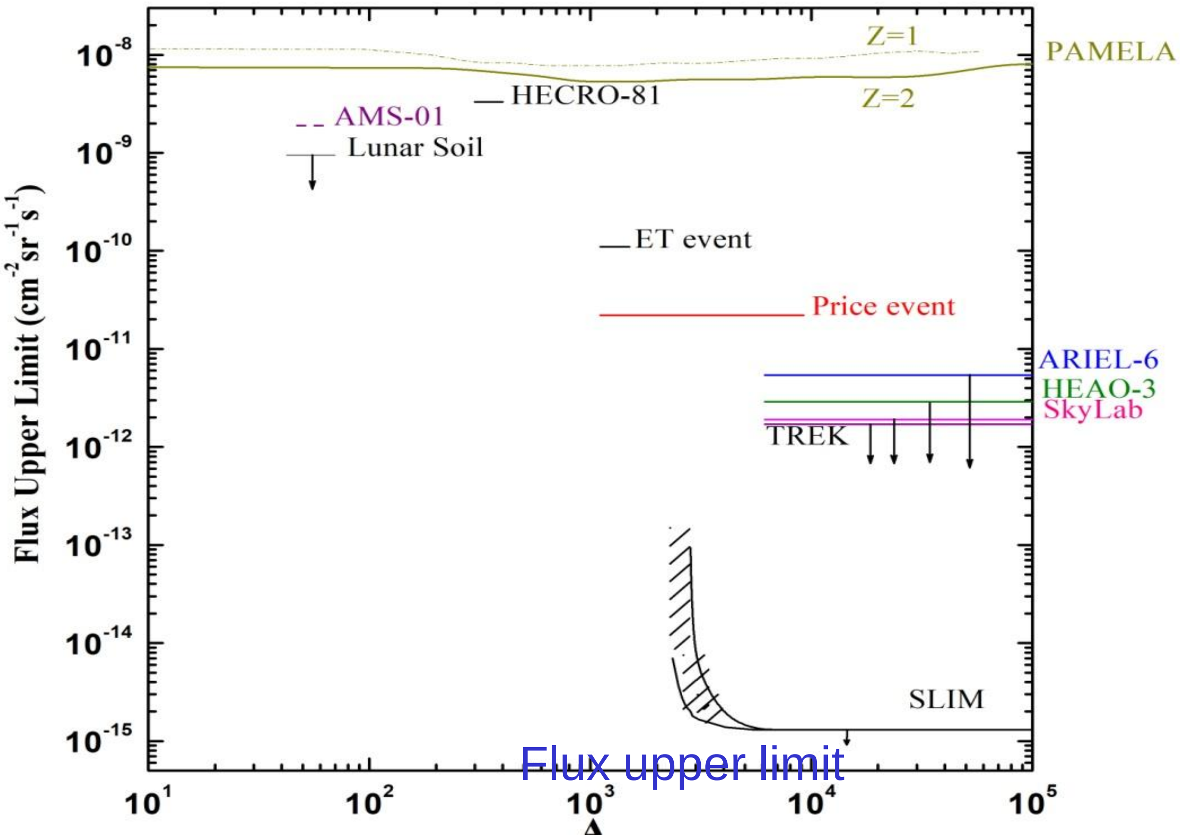

Flux upper limit

Propagation of strangelets through the Earth's atmosphere

Propagation model (1) Wilk et al.

strangelet will continuously lose mass by colliding with atmospheric nuclei until it reaches the critical mass (A = 320) for stable strangelets.

$$A^{final}_{strangelet} = A^{initial}_{strangelet} - A_{air}$$

$$A_{air} = 14.5$$

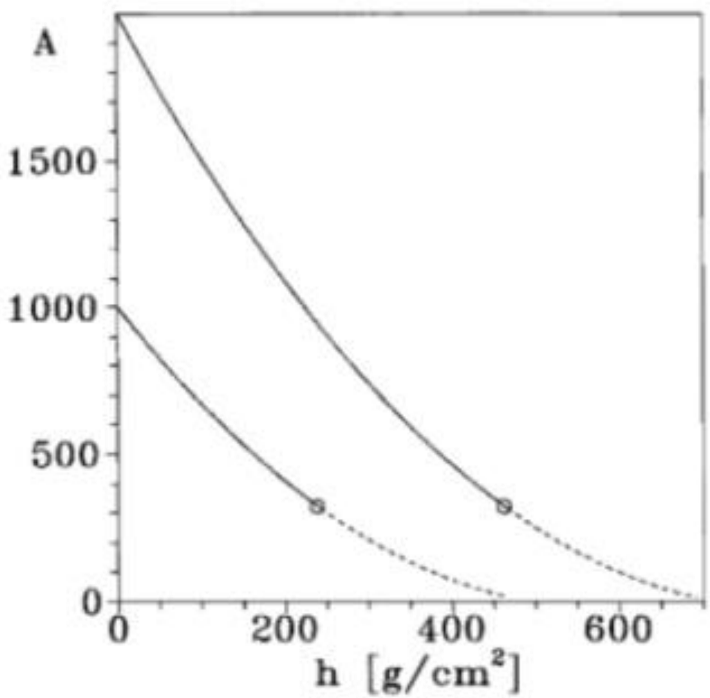

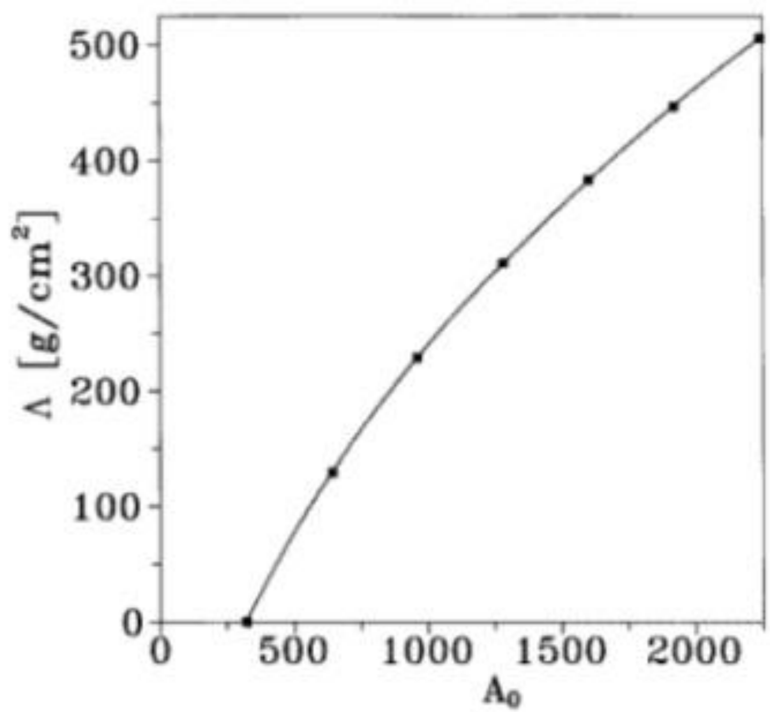

Propagation model (2)Wu et al.

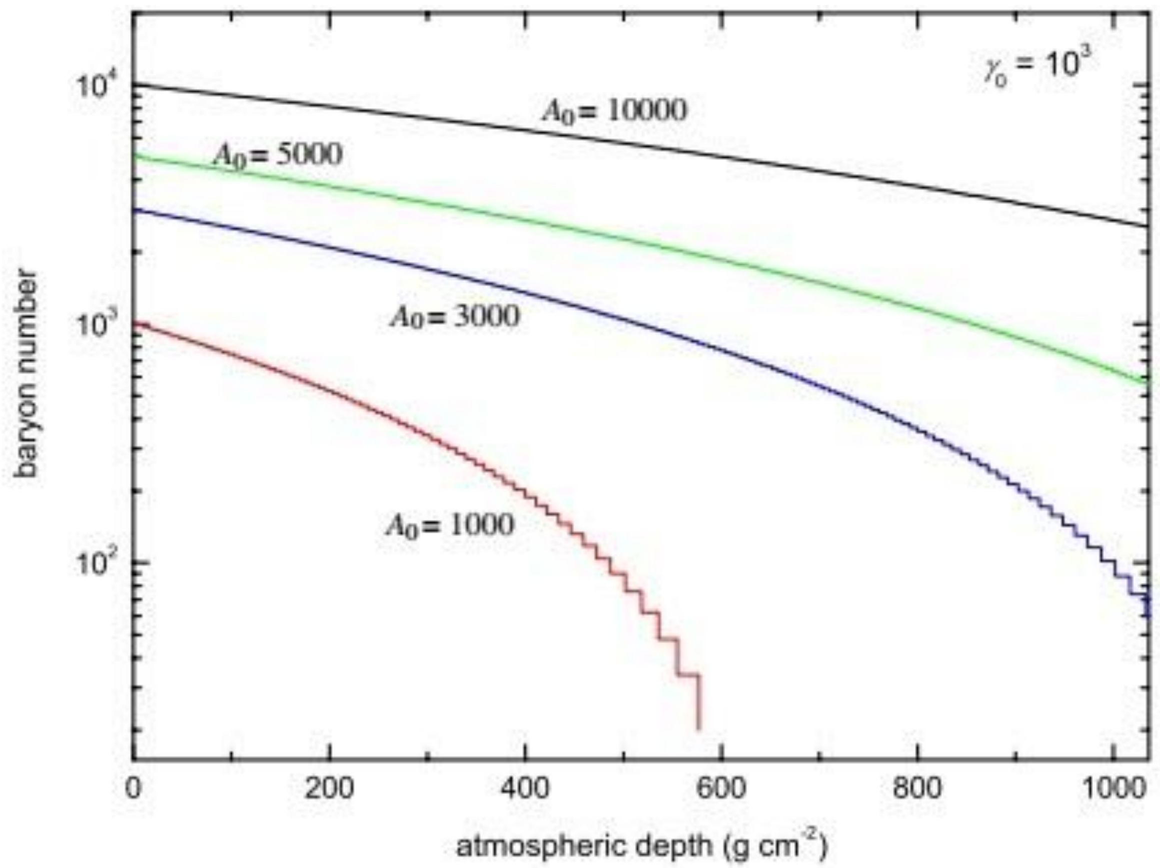

Initially heavy strangelet may reach to the sea level

Prop gation model (3) Banerjee et al.

Initially small strangelet passing through the earth's atmosphere

Gains mass: by preferentially absorbing neutrons over protons from the nuclei of atmospheric atoms

→ Z/A ratio gets even smaller.

β_0	m_{s0}	m_l (amu)	q_l	$\beta_l \times (10^{-3})$	e_l (MeV)
	42	294.7	3	2.8	1.05
0.2	54	369.4	4	3.0	1.55
	60	415.8	4	3.0	1.80
	64	446.5	5	3.1	1.98
	42	246.4	6	4.9	2.84
0.4	54	359.5	8	4.7	3.73
	60	415.6	8	4.7	4.25
	64	452.0	9	4.6	4.63
	42	235.8	10	7.4	5.97
0.6	54	357.1	12	6.6	7.15
	60	416.0	13	6.4	7.87
	64	453.6	14	6.3	8.39
	42	236.4	12	8.6	8.16
0.7	54	359.1	14	7.6	9.59
	60	418.3	15	7.3	10.46
	64	456.3	16	7.2	11.11

searching for strangelets at high altitude

Passive detectors like **Nuclear Tack Detectors (NTDs)** are one of the best choice for experiments that require extended areas and exposures. relatively easy and less-expensive to set up passive detector array.

Some salient features

- Do not need power for their operations or any other in-situ data storage or transmission systems.
- Easy to install
- Suitable for off-line data analysis.
- excellent detection efficiency (almost ~ 100%) within a certain limit (~ $10^4/cm^2$) of the flux of incoming particles
- Can offer good charge, energy and position resolution.
- Intrinsic detection thresholds of some Nuclear Track Detectors (NTDs) provides a natural and easy way of background suppression.

Working principle of Nuclear Track Detectors (NTDs)

Solid State Nuclear Track Detectors are dielectric solids

$$REL = \left(-\frac{dE}{dx}\right)_{electronic}^{E<E_{cut}} = K\left(\frac{z}{\beta}\right)^2\left(\frac{Z}{A}\right)\left[\frac{1}{2}\ln\left(\frac{2m_e c^2\beta^2\gamma^2E_{cut}}{I^2}\right)-\frac{\beta^2}{2}\left(1+\frac{E_{cut}}{E_{max}}\right)-\frac{\delta(\beta\gamma)}{2}\right]$$

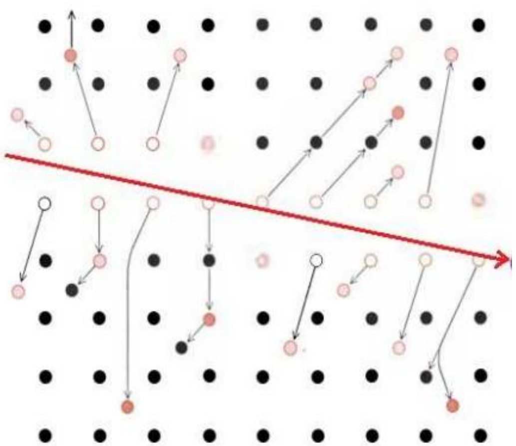

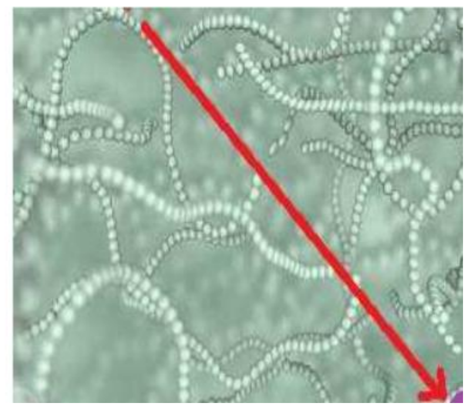

Ionizing particle produces ‘permanent’ damage trail along its direction of motion.
Latent Track (diameter 3-10 nm)

Chemical etching

Damaged region contains more chemically active zones than surrounding undamaged portion.

Applying some chemical reagent (etchant) makes the damaged portion etched out at a faster rate **V_T (Track etch rate)** than the undamaged portion **V_B (Bulk etch rate)**

Geometry of the etch-pit & etch-rate ratio

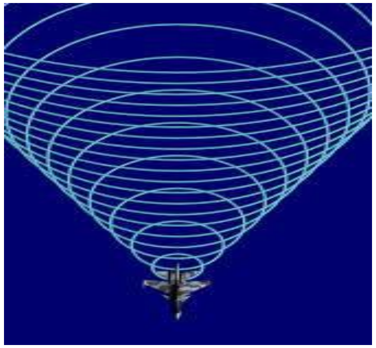

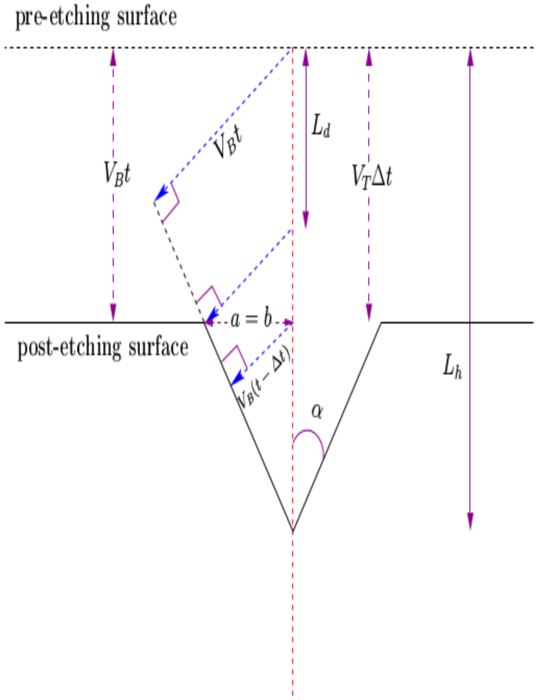

Conical etch-pit

Velocity of the object ⟹ V_T

Velocity of sound ⟹ V_B

Etch-rate ratio:: (V_T/V_B) :: gives a measure of the detector **sensitivity**

$$\frac{V_T}{V_B} = \frac{L_h}{V_B t}$$

$$V_B = \frac{T_i - T_f}{2t}$$

T_i Thickness before etching

T_f Thickness after etching

t Time of etching

Etching continued until the size of the damaged portion increased to ~ µm.

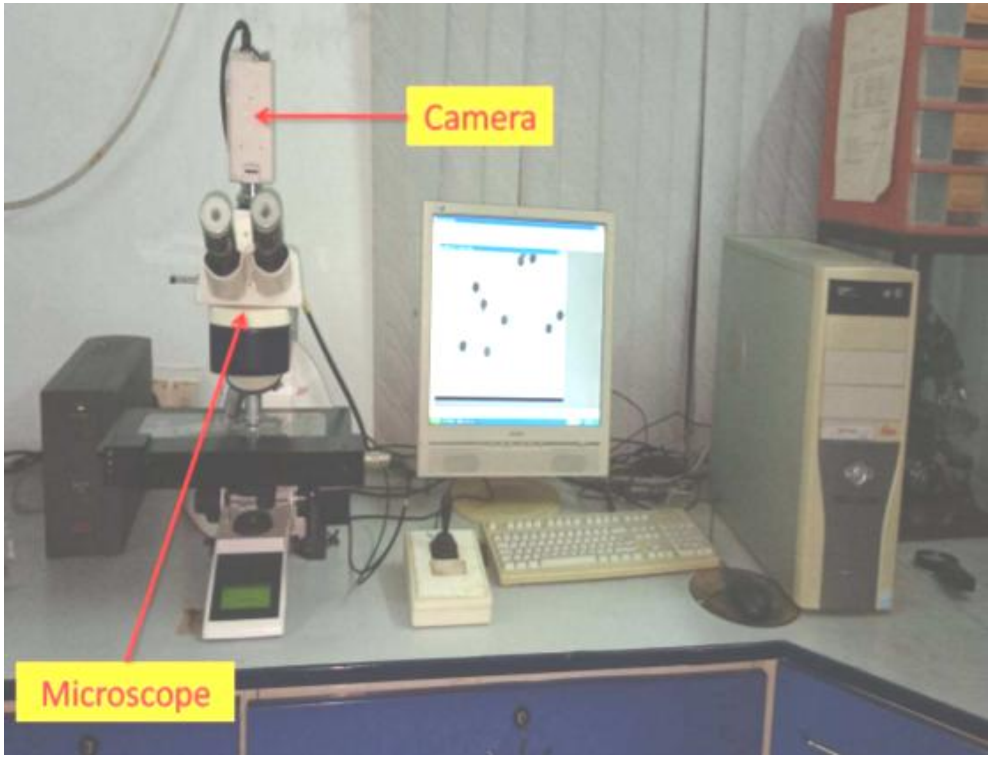

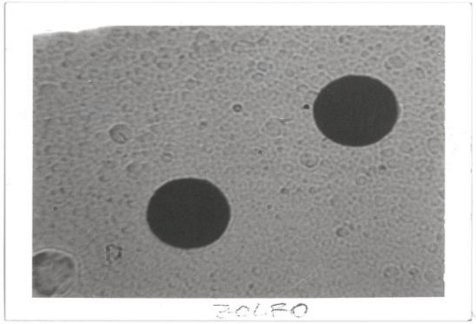

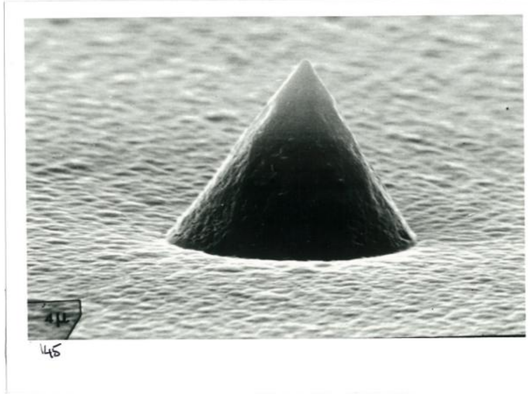

Detection threshold of NTD

Necessary condition for the formation of etch-pit : $\mathbf{V_T/V_B > 1}$

V_T is related with ion's energy loss

Energy loss of the incoming charged particle inside NTDs

$$REL = \left(-\frac{dE}{dx}\right)_{electronic}^{E<E_{cut}} = K\left(\frac{z}{\beta}\right)^2\left(\frac{Z}{A}\right)\left[\frac{1}{2}\ln\left(\frac{2m_e c^2\beta^2\gamma^2 E_{cut}}{I^2}\right) - \frac{\beta^2}{2}\left(1+\frac{E_{cut}}{E_{max}}\right) - \frac{\delta(\beta\gamma)}{2}\right]$$

Detection threshold : minimum value of (z/β) of a particle for which a 'permanent' damage trail is produced by the projectile along its direction of motion.

Determination of the detection threshold of Polyethylene Terephthalate (PET)

Experiment was performed at Ion Beam Laboratory, Institute of Physics, Bhubaneswar, India.

PET (de'Smat, India) and CR-39 (Intercast, Italy) of thickness 100 μm and 700 μm respectively, were cut into pieces (8.5 cm x 1.5 cm)

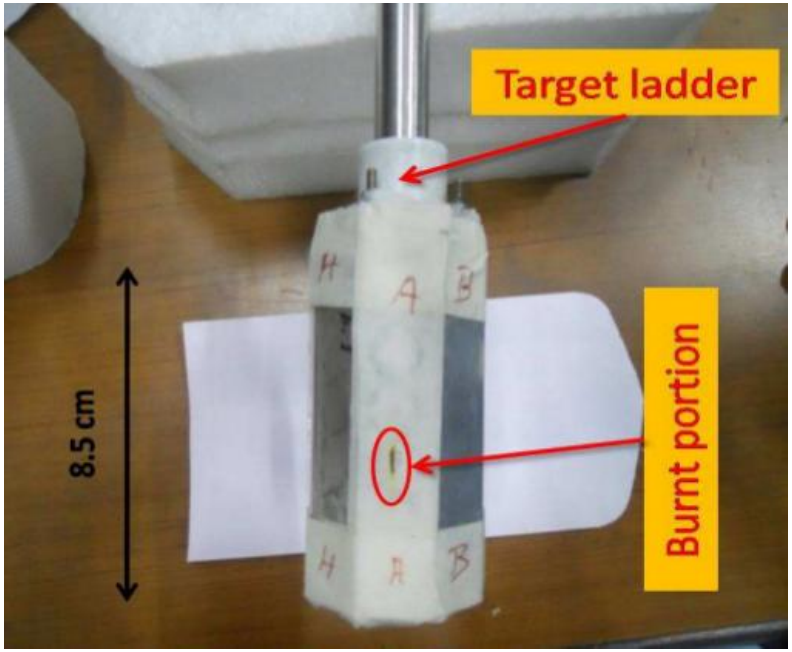

Detectors mounted on the target ladder

Beams used for this experiment

BEAM	ENERGY (MeV)	BEAM CURRENT (nA)	Charge state
PROTON	2	0.6	1
CARBON	11	0.5	4

Etchant and etching condition: 6.25 N NaOH solution at 55.0 ± 0.1 ◦C

Observation using Proton beam

Implies higher detection threshold of PET

No tracks observed on PET

Several tracks observed on CR-39

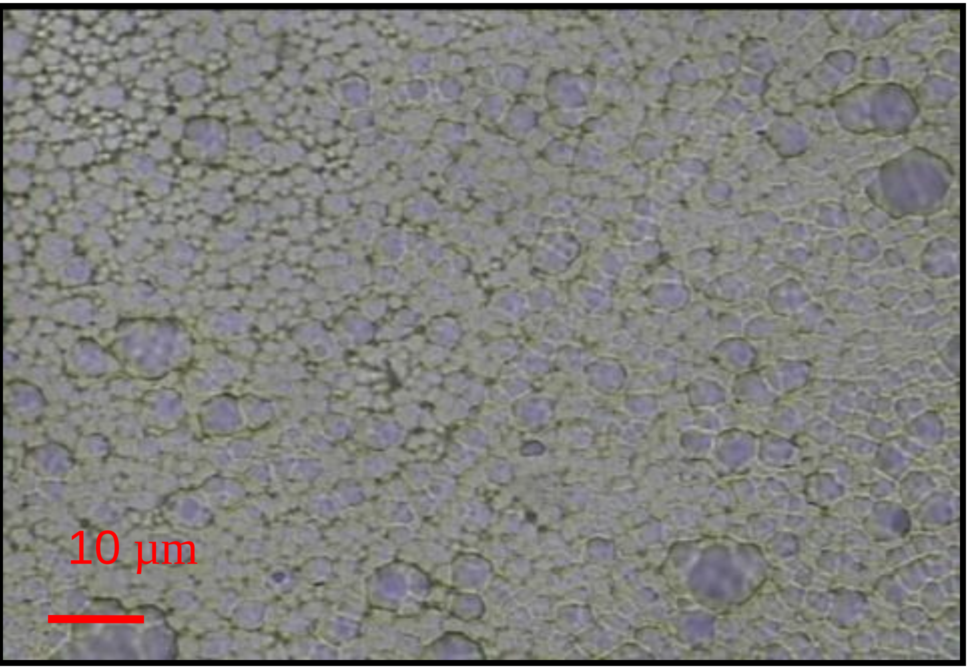

PET irradiated by proton beam after 9 h of etching

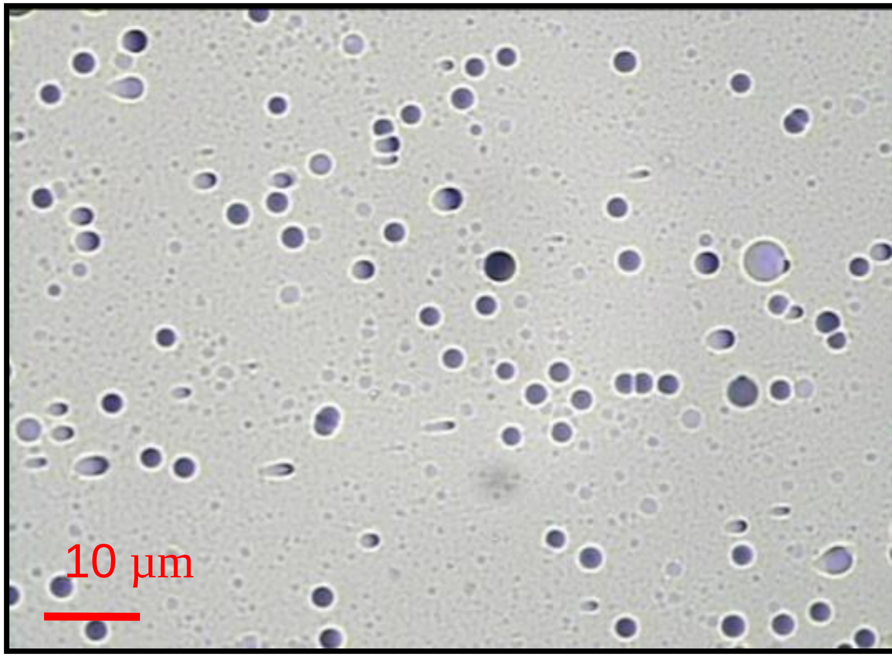

CR-39 irradiated by proton beam after 4 h of etching

Image frames 117 µm x 87 µm, objective100x

Observation using Carbon beam

Track parameters could **not** be measured by existing experimental facility

Etch-pits acquired dimension for measurement using optical microscope

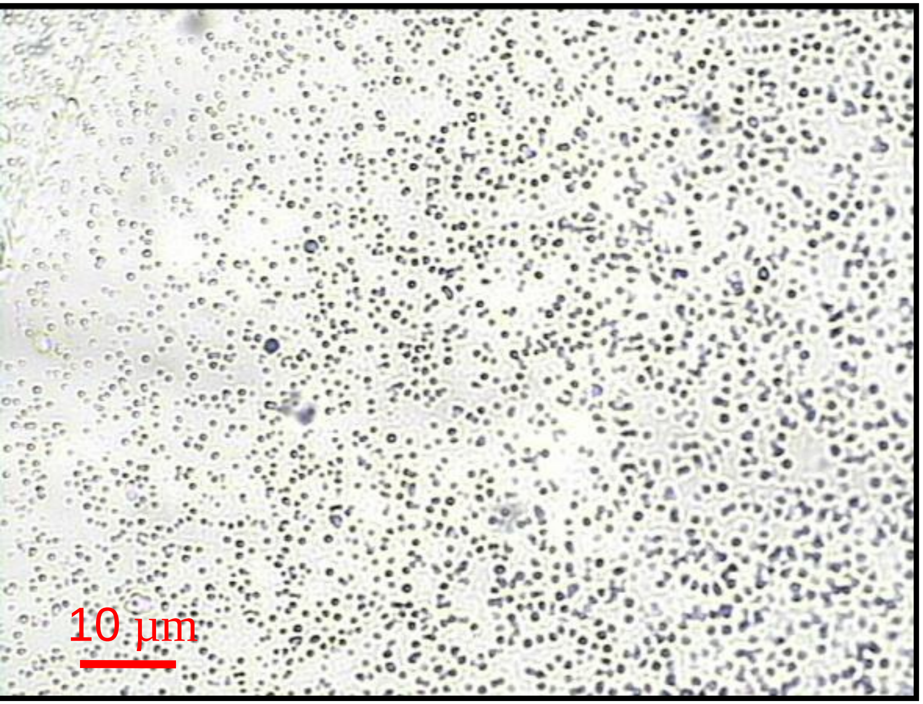

Carbon tracks on PET after 2 h of etching

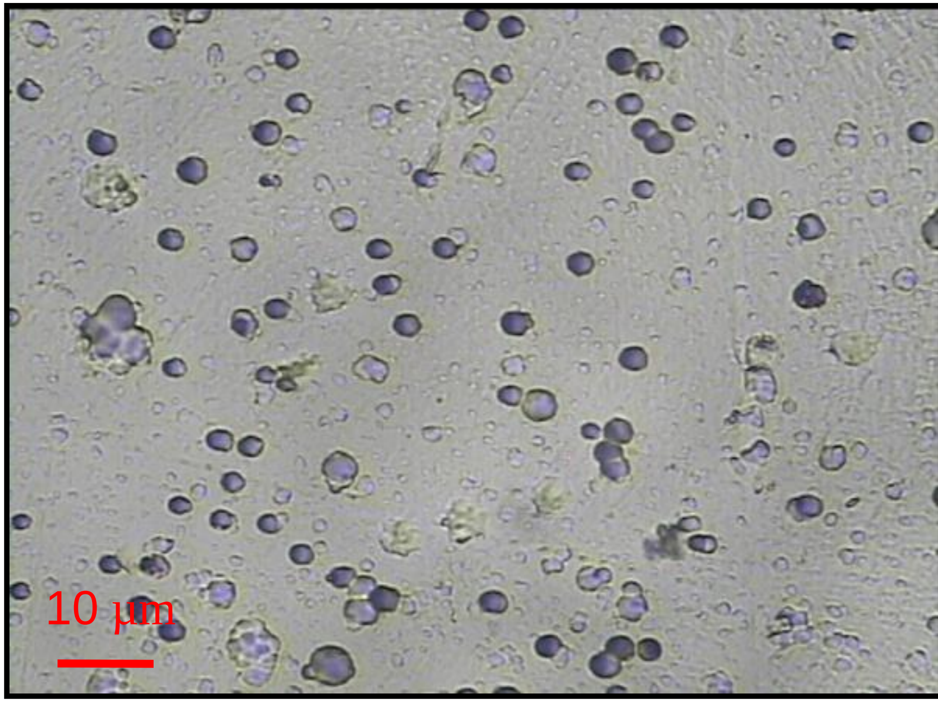

Carbon tracks on PET after 4 h of etching

Image frames 117 µm x 87 µm, objective100x

As the particle penetrates inside the detector, it loses energy.

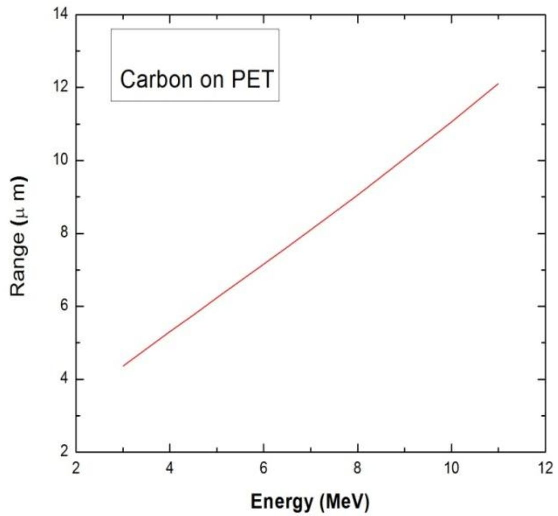

Range computed using SRIM (The Stopping and Range of Ions in Matter)

Duration of etching (h)	Length traversed in PET (μm)	Reduced energy (MeV)	Correspon-ding Z/β
1	1.3	9.74	144
2	2.6	8.43	155
3	3.9	7.08	170
4	5.2	5.68	**190**

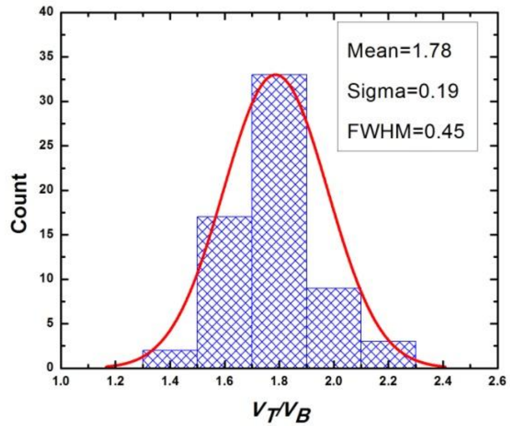

$V_T / V_B = 1.8 \pm 0.5$

Results :

- ❑ Track registration occurs for $\boldsymbol{Z/\beta \geq 140}$ for PET detectors for a specific etchant and etching condition.
- ❑Practical detection threshold (for which the depth of the etch-pit can be measured under existing experimental facility) is found to be $\boldsymbol{Z/\beta \approx 190}$ **which is significantly higher than the traditional NTDs [e.g. CR-39 ($Z/\beta \approx 5$), Makrofol($Z/\beta \approx 50$)].**

Another method for calculating V_T/V_B

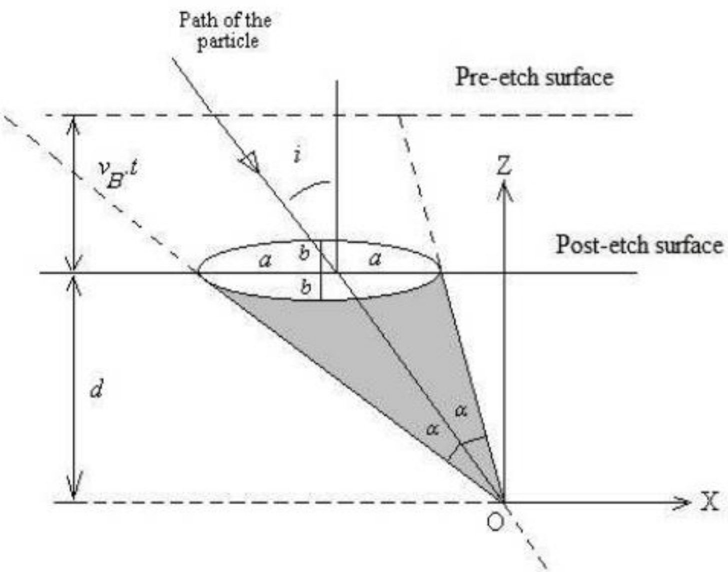

Measurable quantities	Precision of measurement
Depth of the cone [d]	1.0 µm
Major axis diameter[2a]	0.4 µm
Minor axis diameter [2b]	0.4 µm

Depth measurement method

$$\frac{V_T}{V_B} = \frac{V_B t + n d'}{V_B t \cos i}$$

Diameter measurement method

$$\frac{V_T}{V_B} = \sqrt{1 + \frac{4A^2}{\left(1 - B^2\right)^2}}$$

Where,

$$A = \frac{2a}{2V_B t} \quad \text{and} \quad B = \frac{2b}{2V_B t}$$

Advantage of calculating V_T/V_B from diameter measurement method:

- ❑ Better precision
- ❑ Easier focusing of the microscope

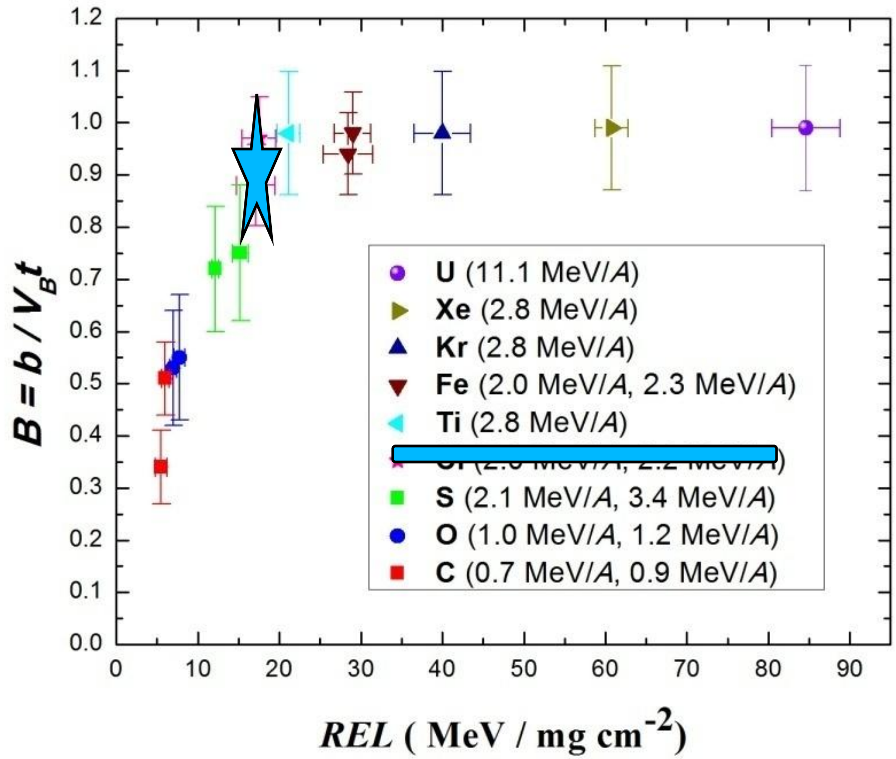

Problem:

Normalised semi-minor axis (B) saturates near B~1

Resulting un-acceptable values of $\mathbf{V_T/V_B}$

Experimental arrangement

Experiment performed at Inter-University Accelerator Center (IUAC), New Delhi

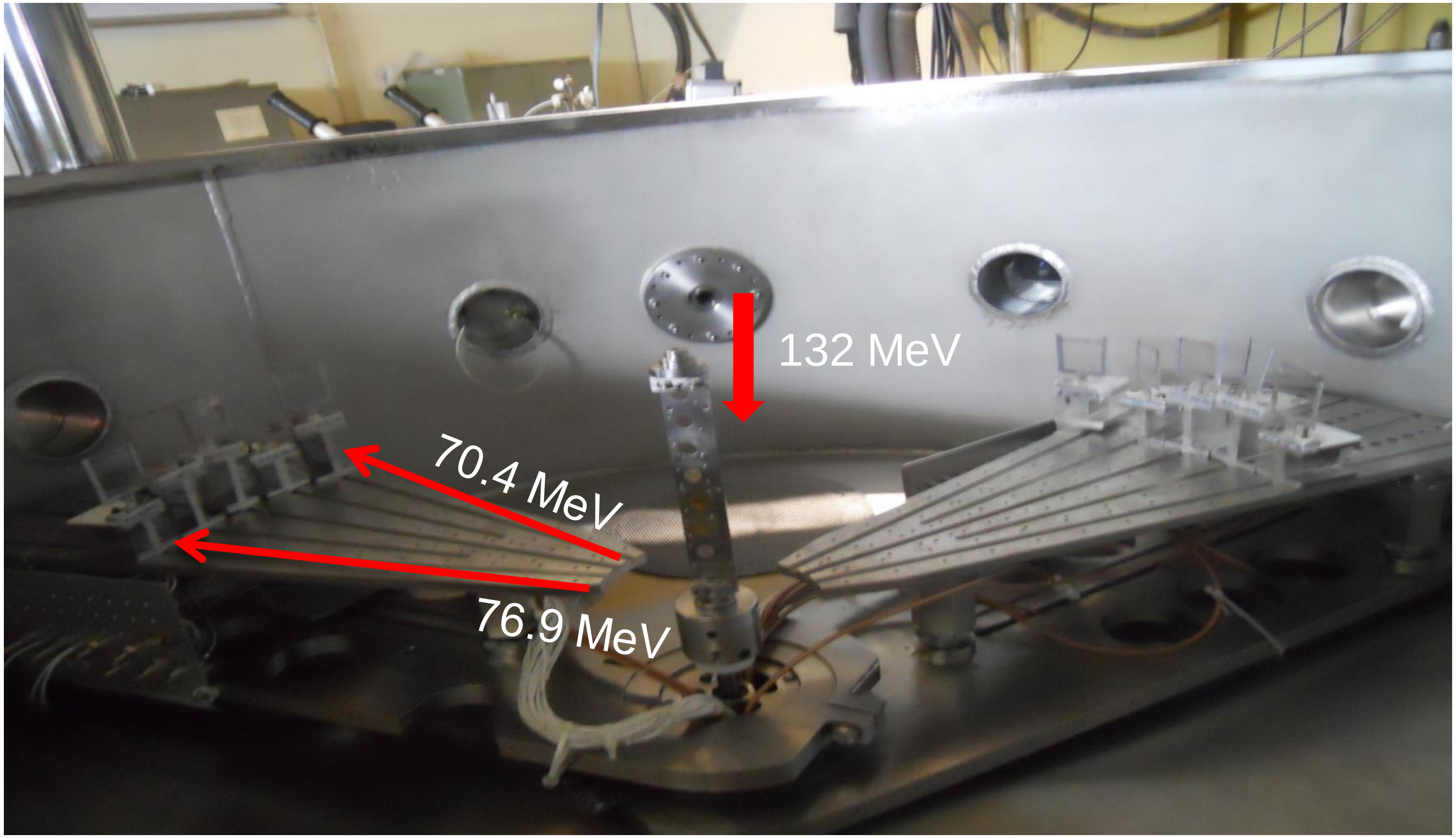

Experimental arrangement

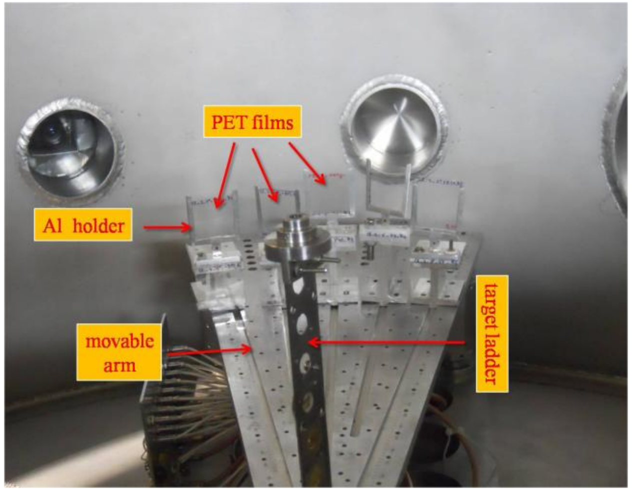

When things go wrong

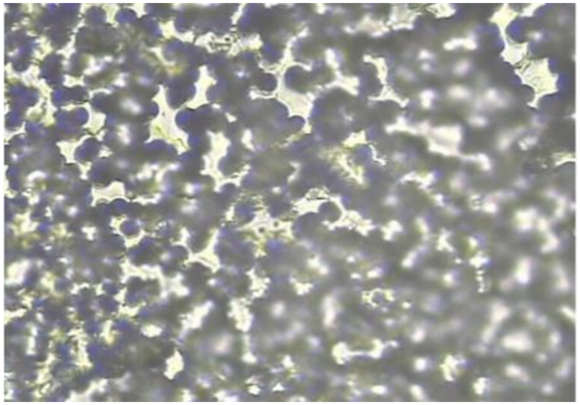

Detector burnout

Ion	Incident energy per nucleus (MeV)	Normalized semi minor-axis *B*	$\frac{V_T}{V_B}$ by depth measurement method	$\frac{V_T}{V_B}$ by diameter measurement method
$^{32}S^{9+}$	67	0.75 ± 0.13	4.5 ± 0.7	3.8 ± 1.3
	110	0.72 ± 0.12	3.7 ± 0.6	3.2 ± 0.9
$^{16}O^{7+}$	16	0.55 ± 0.12	2.7 ± 0.4	2.0 ± 0.5
	20	0.53 ± 0.11	2.3 ± 0.4	1.9 ± 0.4
$^{12}C^{4+}$	8	0.51 ± 0.07	2.1 ± 0.5	1.84 ± 0.25
	11	0.34 ± 0.07	1.8 ± 0.5	1.40 ± 0.12
$^{35}Cl^{10+}$	70	0.97 ± 0.09	5.1 ± 0.5	57 ± 63
	77	0.88 ± 0.08	4.6 ± 0.4	8 ± 5

Applicable *REL* regions for the two method

Calibration curve for PET

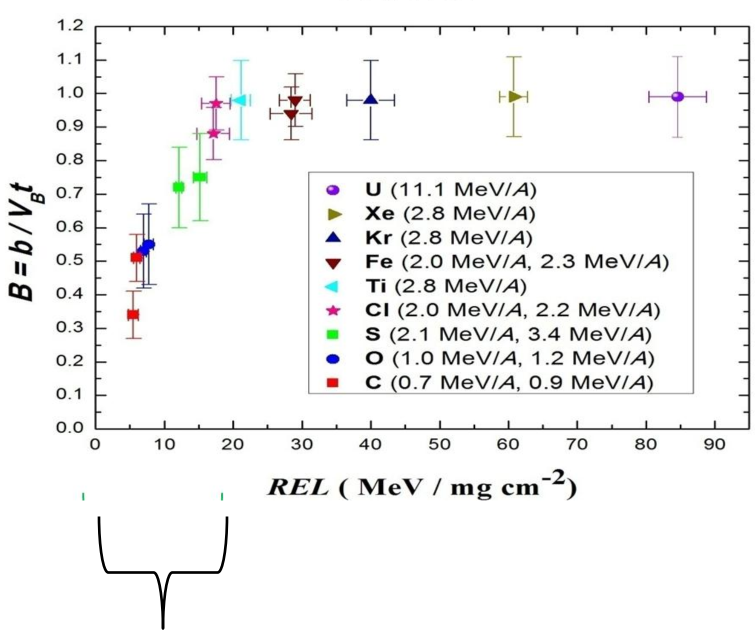

Diameter method

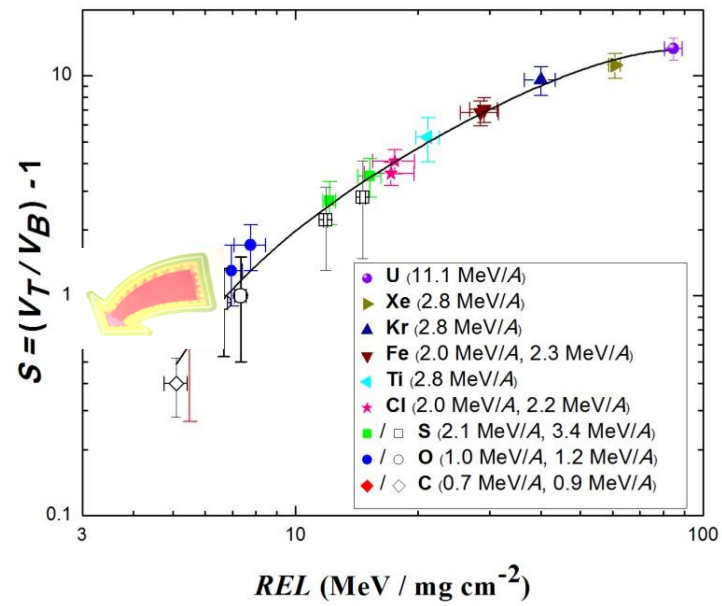

Fit adjusted R^2 is 0.98

Results;

By using both methods the response of PET was determined over a wide range of ions' energy Losses.

Diameter measurement method becomes less sensitive for PET NTD detector when REL ≳ 15 MeV/mg cm $^{-2}$.

Extrapolating the sensitivity function, PET detector's threshold, at REL ≈ 3.5 MeV/mg cm −2 , is derived.

More on detection threshold polymer NTDs

Chart of properties of transparent dielectrics

Name	Density (ρ_m)	Young's modulus (Y)	Specific heat (s)	Thermal conductivity (k_t)	Resistivity (ρ_e)	Detection threshold $(Z/\beta)_{th}$
	(g cm^{-3})	GPa (=10^9 Nm^{-2})	kJ kg^{-1}K^{-1}	W m^{-1}K^{-1}	Ω cm	
CR-39	1.32	2.1	2.3	0.21	2×10^8	6
Cellulose Acetate	1.30	2.4 –4.1	1.45 –1.51	0.167 –0.335	(3.3 –30) x10^{12}	40
Lexan	1.20	2.2	1.26	0.195	1x10^{17}	57
PET	1.38	2.8 –3.1	1	0.15 –0.24	5×10^{18}	140-190
Perspex	1.19	3.21	1.4 –1.5	0.17 –0.19	8×10^{15}	?

Ref: *Properties of polymers - Their correlation with chemical structure* (fourth edition) - D. W. van Krevelen and Klaaste Nijenhuis.

Heat equation $$\frac{\partial \theta}{\partial t} = h\nabla^2\theta$$

h Thermal diffusivity

Diffusion equation $$\frac{\partial n}{\partial t} = D\nabla^2 n$$

D Diffusion constant

Parameter	$(Z/\beta)_{th}$	Reason
h increases	Increases	Higher ***h*** ⟹ Quicker 'fading' of a track plastic film is dipped in an etchant solution at a relatively higher temperature
D increases	Decreases	Higher ***D*** ⟹ Removal of the electrons produced during track formation, from the vicinity of the track would help in the preservation of the track

$$(Z/\beta)_{th} \sim f\left(\frac{h}{D}\right)$$

h/D is a dimensionless quantity

Mobility equation:

$$\frac{D}{\mu} = \frac{kT}{e}$$

Now, $$h = \frac{k_t}{\rho_m s}$$

So, $$\frac{h}{D} = \frac{ek_t}{\rho_m skT\mu}$$

$$(Z/\beta)_{th} \sim f\left(\frac{ne^2 k_t}{\rho_m skT} . \rho_e\right)$$

$$(Z/\beta)_{th} \sim F(\rho_e)$$

Guess : power law

$$(Z/\beta)_{th} \sim (\rho_e)^q$$

So,

$$\ln(Z/\beta)_{th} = q\ln(\rho_e) + c\ .$$

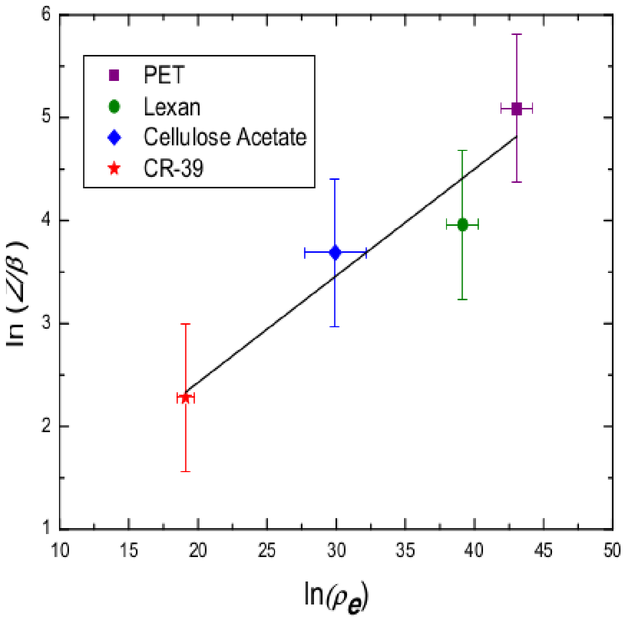

Fit adjusted R^2 is 0.87

$\ln(Z/\beta)_{th} = q\ \ln(\rho_e) + c$

q = 0.12 ± 0.02 and

c = - 0.47 ± 0.77

Name	Predicted $(Z/\beta)_{th}$
Perspex	59±6

Experimental determination of the Detection threshold of Perspex

Perspex irradiated with alpha from Am^{241} in vacuum at VECC,India for 1h.

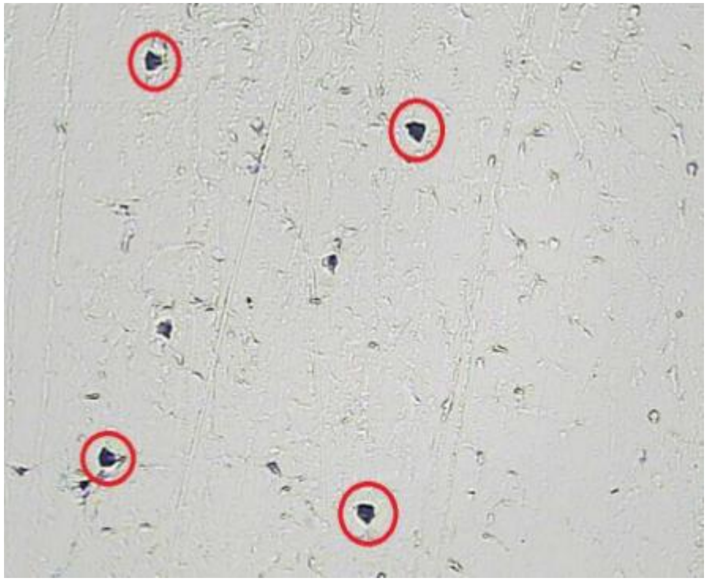

Alpha tracks on Perspex after 2 h etching using 6.25 N NaOH at 70^0C

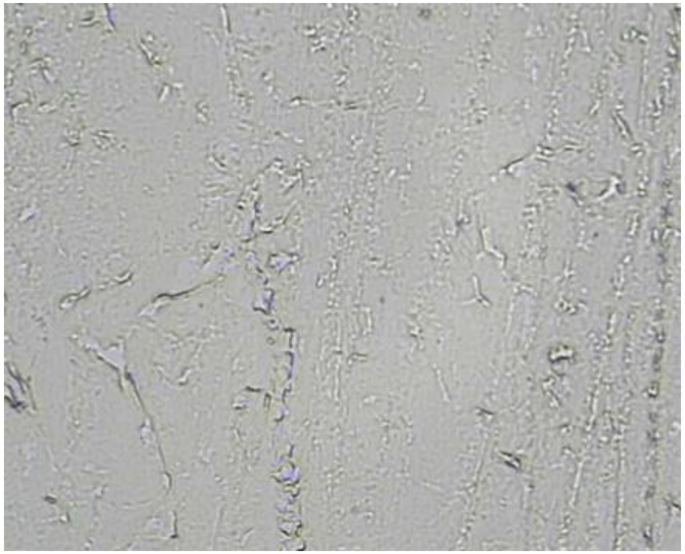

Unexposed region of Perspex

The size of the image frames are 117 µm x 87 µm.

Duration of etching (h)	Length traversed in Perspex(µm)	Reduced energy (MeV)	Corresponding Z/β
0	0	5.5	37
2	21±07	$2.9^{+1}_{-1.3}$	50^{+16}_{-7}

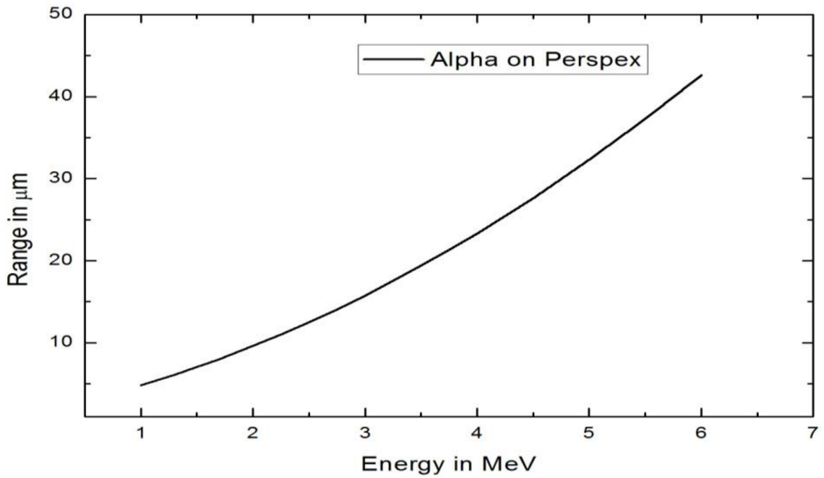

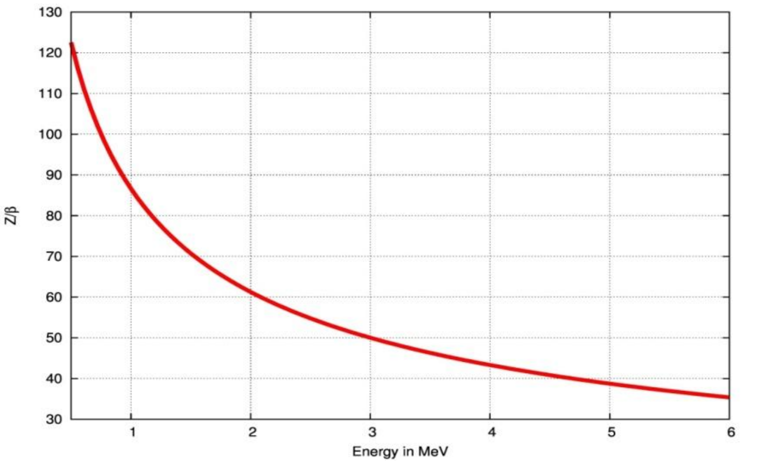

Range vs energy for alpha on Perspex computed using SRIM

(Z/β) vs energy for alpha on Perspex

Name	Predicted value of $(Z/\beta)_{th}$	Measured value of $(Z/\beta)_{th}$
Perspex	59±6	50^{+16}_{-7}

Study of radiation background at various high altitude locations

Goal :

- To check the changes detector behaviour with exposure to harsh environmental conditions
- To survey the local radiation background.

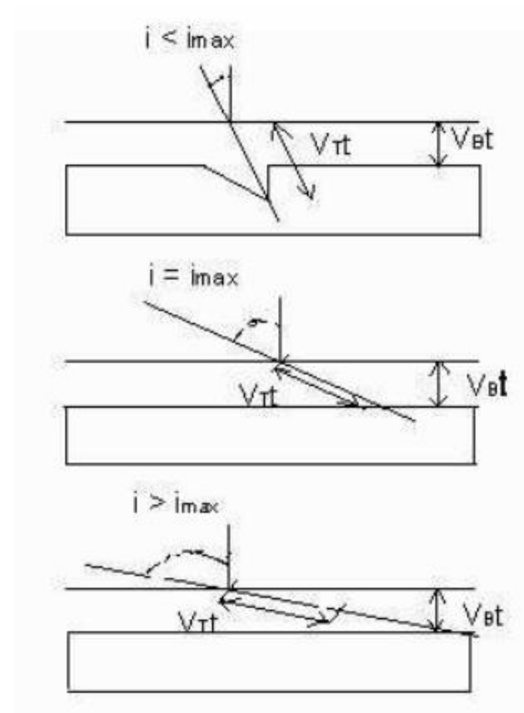

Geometric acceptance of NTD

3 PET films of A4 size (297 mm x 210 mm) and thickness 90 µm as well as CR-39 films of size (5 cm x 5 cm) and thickness 700 µm were mounted on Perspex stands and given open air exposures.

Site chosen for the pilot study

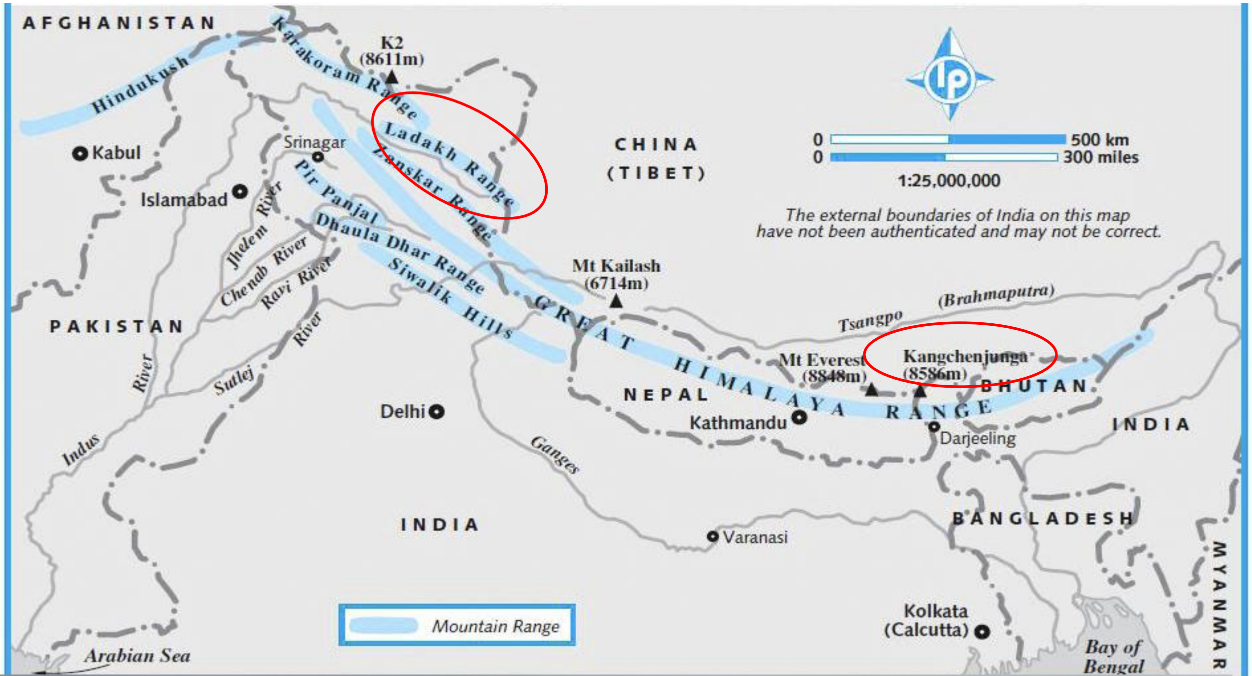

Some parameters of the exposure sites

Place	Altitude (a.m.s.l.) [m]	Atmospheric Depth [g cm^{-2}]	Geographic latitudes and longitudes	Geomagnetic latitudes and longitudes	Geomagnetic cut off rigidity [GV]
Darjeeling	2200	795	27.0º N, 88.3º E	17.6º N, 162.2º E	14.7
Ooty	2200	800	11.4º N, 76.7º E	2.9º N, 149.9º E	15.9
Hanle	4500	591	32.8º N, 75.9º E	24.2º N, 151.2º E	14.2

Footprint of cosmic rays on CR-39

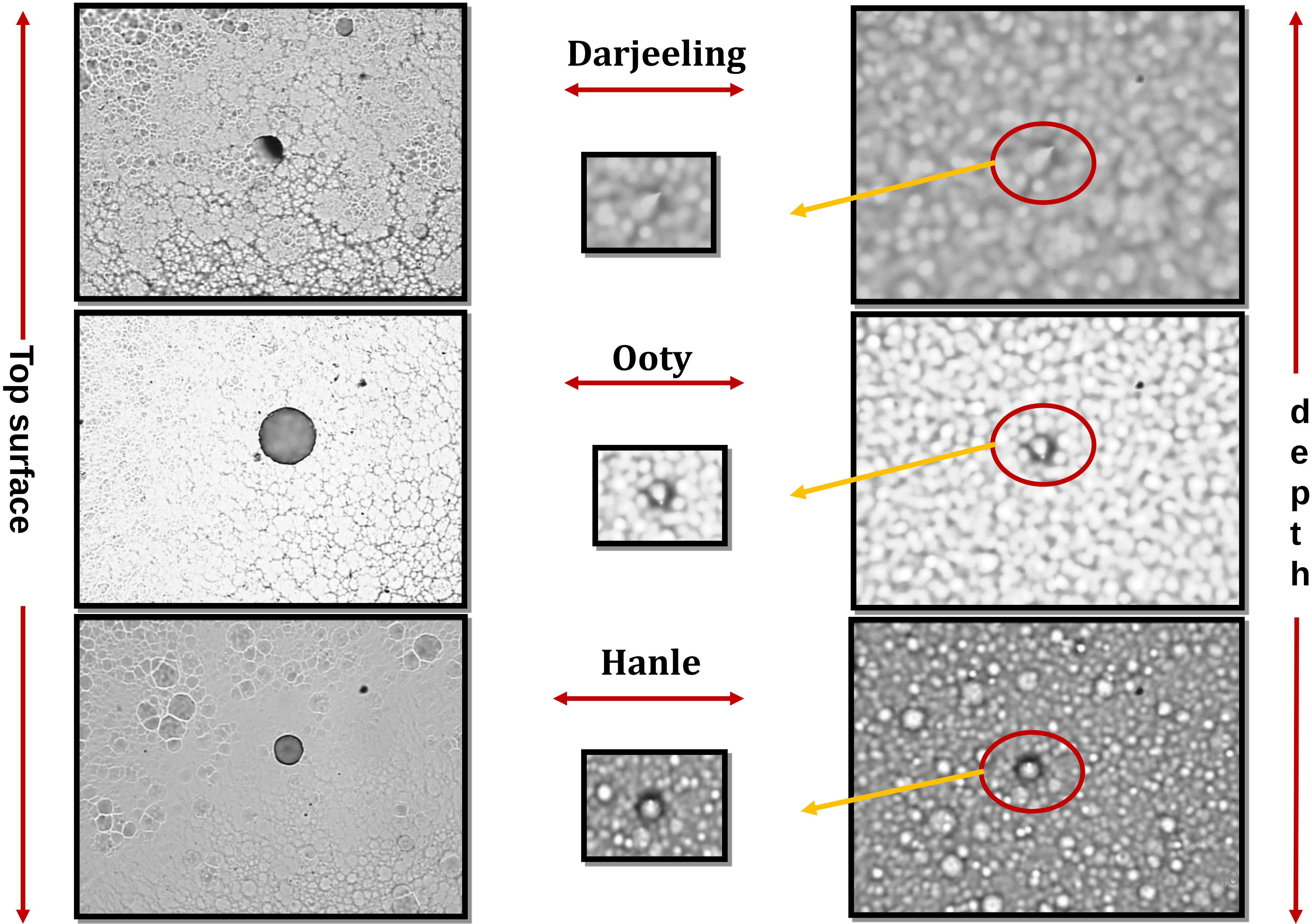

Distribution of tracks recorded on CR-39 at Darjeeling, Ooty and Hanle

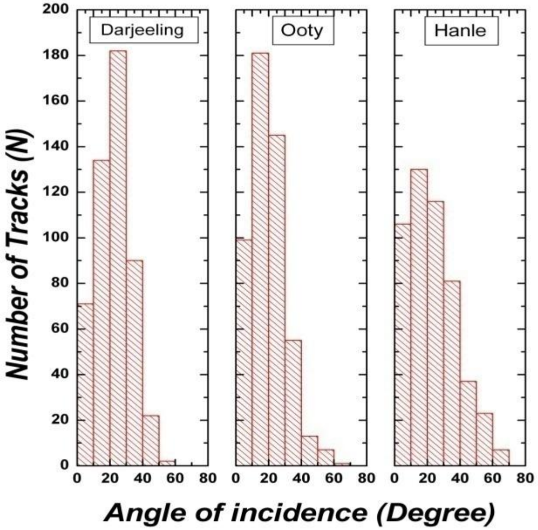

Distribution of the angle of incidence

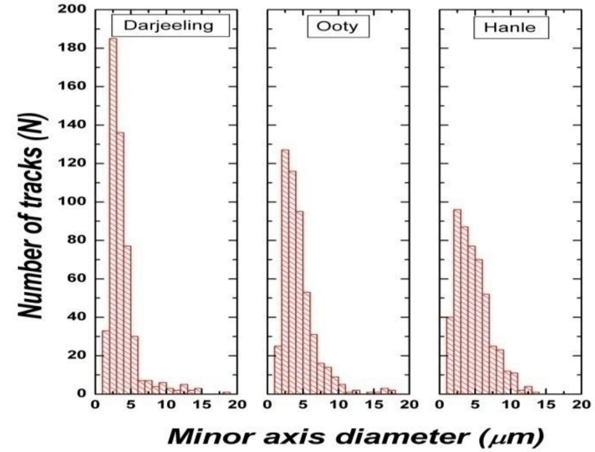

Distribution of the minor axis

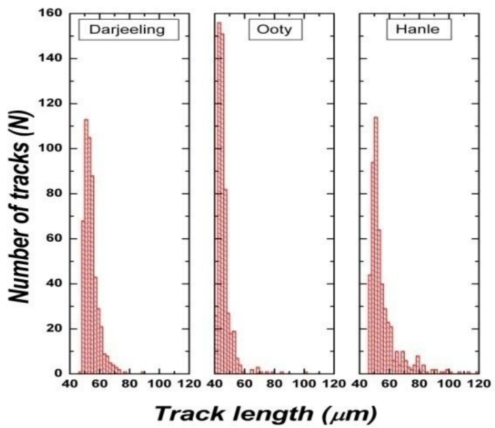

Distribution of the track length

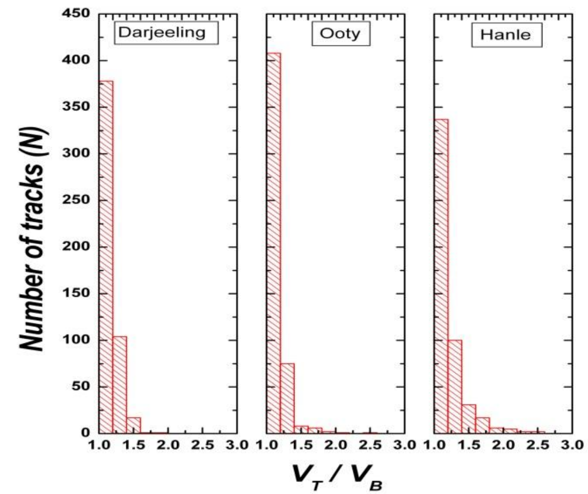

Distribution of the V_T / V_B

Bulk etch rates of CR-39 and PET

Place	Exposure Duration (Days)	V_B of CR-39 (µm/h)	V_B of PET (µm/h)
Darjeeling	532	11.7 ± 0.7	2.6 ± 0.15
Ooty	190	10.0 ± 0.6	2.2 ± 0.13
Hanle	320	11.5 ± 0.7	2.4 ± 0.13
Unexposed	-	1.4 ± 0.07	1.0 ± 0.05

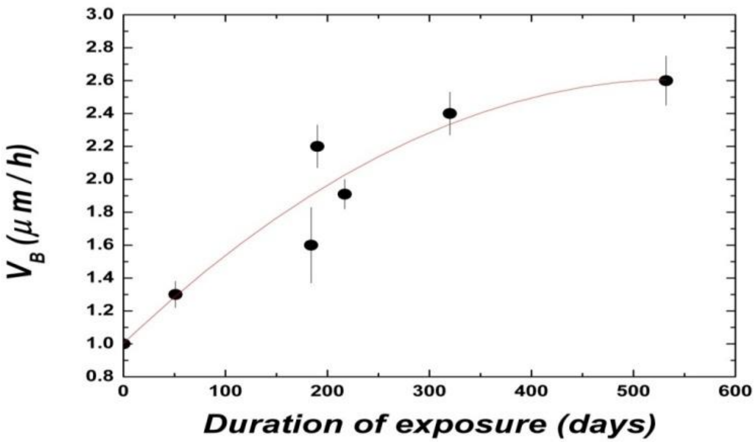

Variation in the bulk etch rates with the duration of exposure of PET

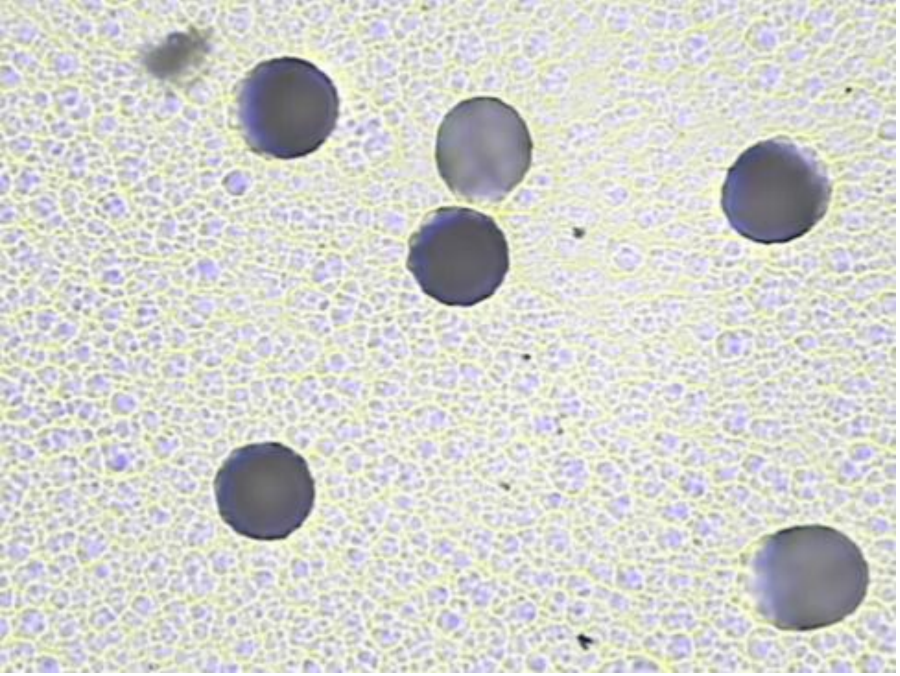

Etch-pits seen on CR-39 exposed at Darjeeling after 4 h etching.
image frame 117 μm × 87 μm

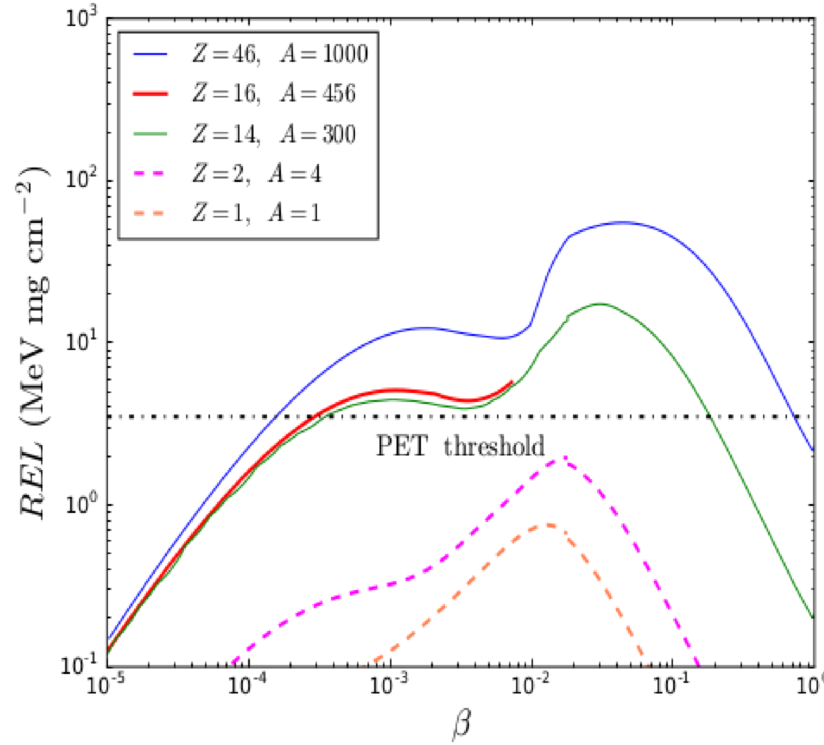

Strangelet on PET

Place	Flux of background on CR-39 ($cm^{-2}\ s^{-1}\ sr^{-1}$)	Flux on PET ($cm^{-2}\ s^{-1}\ sr^{-1}$)
Darjeeling	6.0×10^{-4}	$< 1.0 \times 10^{-11}$
Ooty	1.3×10^{-4}	$< 4.1 \times 10^{-11}$
Hanle	4.6×10^{-4}	$< 2.4 \times 10^{-11}$

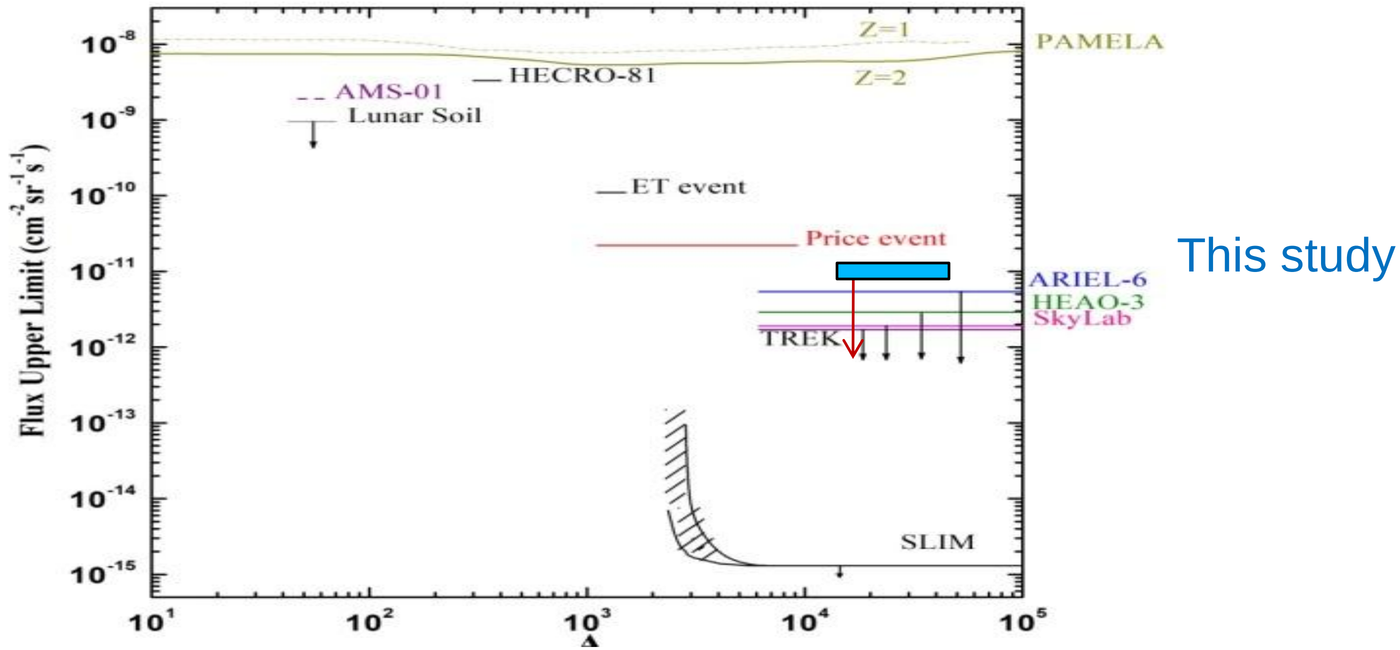

Results:

- Local radiation background and change in the detector responses in different weather conditions have been surveyed.
- It is found that the PET detectors are comparatively more robust with respect to the change in bulk etch-rate.
- PET films retain their flexibility
- It is also observed that PET is efficiently eliminating the low ionizing background and thus they are particularly suited for the search of rare, highly ionizing particles against a large background from weakly ionizing particles

Conclusions

- It has been established that the detection threshold of PET is significantly higher than the detection thresholds of many other commonly used NTDs.
- Two widely used methods of determining the etch-rate ratio in NTDs , based on the size of etch pit‘s surface opening and depth, respectively - are compared in different regimes of ions’ energy loss.
- A calibration curve is obtained for PET .

Through this sequence of studies of its characteristics, we are able to establish a particular brand of PET as a high threshold, rugged and competent candidate for an NTD.

- Open-air exposures at different high altitude locations ensures the ruggedness of the PET detector.
- Pilot studies also reflects the efficiency of high threshold PET detectors in eliminating the huge low ionizing background from weakly ionizing particles red. and thus they are particularly suited for the search of rare, highly ionizing particles.
- We are planning to make a 100 m^2 array to search for the highly ionizing rare events in cosmic rays. e.g. According to Banerjee model expected strangelet flux at an altitude of 3000 m is $\sim 10^{-12}\ cm^{-2}\ s^{-1}\ sr^{-1}$. So with one year exposure we should have about 100 events. This proposed array with NTD may be helpful to study other strangelet propagation models and look for other rare events in cosmic rays as well.

Publications

1) *A comparative study of alternative methods to determine the response of poly-ethylene terephthalate nuclear track detector* R. Bhattacharyya, S. Dey, Sanjay K. Ghosh, Akhil Jhingan, A. Maulik, L. Patrizii, Sibaji Raha, D. Syam and V. Togo **Nuclear Inst. and Methods in Physics Research B 434 (2018) 51-55.** doi: 10.1016/j.nimb.2018.08.001

2) *Comparison of charge response of PET films of different brands used as high threshold Nuclear Track Detectors* Sayantan Bhattacharya, R. Bhattacharyya, S. Dey, Sanjay K. Ghosh, Akhil Jhingan, A. Maulik, Sibaji Raha and D. Syam, **Radiation Measurements 119 (2018) 166–169**.d oi: 10.1016/j.radmeas.2018.10.013

3) *Study of radiation background at various high altitude locations in preparation for rare event search in cosmic rays*, R. Bhattacharyya, S. Dey, Sanjay K. Ghosh, A. Maulik, Sibaji Raha, D. Syam ***Journal of Cosmology and Astroparticle Physics*** 2017 (04) 035

4) *Determination of the detection threshold for Polyethylene Terephthalate (PET) Nuclear Track Detector (NTD),* R. Bhattacharyya, S. Dey, Sanjay K. Ghosh, A. Maulik, Sibaji Raha, D. Syam ***Nuclear Instruments and Methods in Physics Research B*** 2016 (370) 63-66

Acknowledgement

Funding agency : IRHPA (Intensification of Research in High Priority Areas) Project of the Department of Science and Technology, Government of India,.

Group members: Sandhya Dey, Sanjay K. Ghosh, Atanu Maulik, Sibaji Raha, Debapriyo Syam

Very special thanks to Dr. Laura Patrizii for giving me the opportunity to work at INFN, Bologna and to Professor JamesPinfold for providing the support during my stay.

GRAZIE MILLE


thank you!

Particle identification scheme at a glance

Calibration of the detector:

i.Exposing the detector with ions of known Z & E.
ii.Experimentally finding the value of Vt/Vb from track parameters.
iii.Finding the corresponding value of dE/dX and R from simulation using SRIM software.
iv.Making a calibration curve of dE/dX vs. Vt/Vb.
v.Making a reference curve of dE/dX vs. Range using SRIM software.

For the detection of a unknown particle :

1.Experimentally finding the value of Vt/Vb & Range from track parameters of the corresponding track.
2.Finding corresponding dE/dX (from iv).
3.Finding the Atomic no. (Z) from v.
4.Using this value of Z, Finding the Energy of the particle for the corresponding Range.